

27P

N63-10537

CODE 1.

NASA TN D-1517

NASA TN D-1517



TECHNICAL NOTE

D-1517

HOVERING CHARACTERISTICS OF A ROTOR HAVING
AN AIRFOIL SECTION DESIGNED
FOR A UTILITY TYPE OF HELICOPTER

By James P. Shivers and William J. Monahan

Langley Research Center
Langley Station, Hampton, Va.

NATIONAL AERONAUTICS AND SPACE ADMINISTRATION
WASHINGTON

December 1962

NATIONAL AERONAUTICS AND SPACE ADMINISTRATION

TECHNICAL NOTE D-1517

HOVERING CHARACTERISTICS OF A ROTOR HAVING
AN AIRFOIL SECTION DESIGNED
FOR A UTILITY TYPE OF HELICOPTER

By James P. Shivers and William J. Monahan

SUMMARY

An investigation has been conducted on the Langley helicopter test tower to determine the hovering performance characteristics of a rotor having an NACA 63₁A012 airfoil thickness distribution in combination with an NACA 130 mean line. The results of this investigation are compared with data from a previously investigated rotor having an NACA 63₂A015 airfoil thickness distribution in combination with an NACA 230 mean line. The purpose of this comparison is to determine the magnitude of improvement in hovering performance for the present rotor compared with the previous rotor for tip Mach numbers above 0.50. It was found that the thinner airfoil with less camber, as used in a rotor, does provide a material increase in efficiency at tip Mach numbers above 0.50. The geometry of the rotor blades is essentially the same except for the thickness ratio and camber.

The hovering performance of the rotor with a distributed type of leading-edge roughness is compared with that of other 12- and 15-percent-thick rotor blades that have similar roughness conditions. This comparison shows that the rotor of this investigation, with leading-edge roughness, operates 2 to 15 percent more efficiently than the other rotors at a mean lift coefficient of 0.5.

INTRODUCTION

This paper presents the results of research relating to improving the rotor hovering efficiency of a utility type of helicopter. This study is an extension of efforts to determine a good compromise for rotor blade airfoil geometry. It is desired to obtain a rotor blade that produces high efficiencies through an extended tip speed range and also to have minimum profile-drag losses at high tip speeds. The rotor blade of reference 1 with an NACA 63₂-015 airfoil section exhibited the best hovering performance characteristics of any rotor that had, up to that time, been investigated on the Langley helicopter test tower. As a result of these findings, a rotor blade having a 15-percent thickness ratio and an NACA 6A-series thickness distribution (A-series used for ease of construction; see refs. 2 and 3) in conjunction with an NACA 230 mean line was investigated as a suitable airfoil for a load-lifter type of helicopter. (See ref. 4.) The profile-drag losses on

this airfoil at tip Mach numbers above 0.6 were such that they canceled the gains in efficiency obtained by the use of camber. Although operating characteristics at tip Mach numbers above 0.6 are of little importance for a load lifter, they are of significance for the utility type of helicopter. For this reason, it was decided to investigate an NACA 6A-series airfoil with a 12-percent thickness ratio in conjunction with an NACA 130 mean line. Other parameters were held constant.

This paper compares the performance efficiency of these two rotors. The basic performance characteristics were obtained with the rotor blades smooth and also with varying degrees of leading-edge roughness. The rotor blades were tested on the Langley helicopter test tower to determine the force data over a range of tip Mach numbers from 0.28 to 0.75 with corresponding blade tip Reynolds numbers from 1.53×10^6 to 4.16×10^6 .

SYMBOLS

b	number of blades
c	blade chord at radius r, ft
$c_{d,o}$	airfoil-section profile-drag coefficient
c_e	equivalent blade chord, $\frac{\int_0^R cr^2 dr}{\int_0^R r^2 dr}$ (on thrust basis), ft
c_l	airfoil-section lift coefficient
\bar{c}_l	rotor blade mean lift coefficient, $6C_T/\sigma$
c_t	blade chord at tip, ft
C_m	rotor blade pitching-moment coefficient, $\frac{M_Y}{\frac{R\rho}{2}(\Omega R)^2 c_e^2}$
C_Q	rotor torque coefficient, $\frac{Q}{\pi R^2 \rho (\Omega R)^2 R}$
$C_{Q,o}$	rotor profile-drag torque coefficient, $\frac{Q_o}{\pi R^2 \rho (\Omega R)^2 R}$

C_T	rotor thrust coefficient, $\frac{T}{\pi R^2 \rho (\Omega R)^2}$
M_t	rotor blade tip Mach number
M_Y	rotor blade pitching moment, lb-ft
N_{Re}	Reynolds number at blade tip, $\frac{\rho \Omega R c_t}{\mu}$
Q	rotor torque, lb-ft
Q_0	rotor profile-drag torque, lb-ft
r	radial distance to a blade element, ft
R	rotor blade radius, ft
T	rotor thrust, lb
α_r	blade-section angle of attack, deg or radians, as specified
θ	blade-section pitch angle measured from line of zero lift at 0.75R or tip, as specified, deg
μ	coefficient of viscosity, slugs/ft-sec
ρ	mass density of air, slugs/cu ft
σ	rotor solidity, $b c_e / \pi R$
Ω	rotor angular velocity, radians/sec
Subscript:	
t	at blade tip

The figure of merit is equal to $0.707 C_T^{3/2} / C_Q$.

APPARATUS AND TESTS

Rotor Blades

The rotor used for this investigation was a fully articulated, two-blade rotor with flapping hinges located at the center of rotation and drag hinges located at the 5.35-percent spanwise station.

A photograph of a typical installation on the Langley helicopter test tower is shown in figure 1. A sketch with pertinent blade dimensions is presented in figure 2. The rotor solidity was 0.032, the blade radius was 18 feet, the pitch axis was located at 0.23c, and the twist distribution was as indicated in figure 2. The blade chordwise center of gravity was fairly uniform radially, and the effective value was about 24.5 percent. Approximately the outer 60 percent of the rotor blade was contoured to an NACA 63₁A012 airfoil thickness distribution in combination with an NACA 130 mean line (designated in fig. 2 as NACA 63₁A012 (130 mean line) airfoil section). The stations and ordinates for the airfoil are given in table I. The airfoil surface was smooth and fair over the entire blade.

In order to determine the extent to which the rotor performance would be affected by a distributed type of leading-edge roughness, tests were made with various conditions of roughness which are described more specifically in a subsequent section of this paper.

Experimental Methods and Accuracy

The experimental procedure was the same as that of references 4 to 7 in that the blades were rotated in hovering for a series of rotor tip speeds at various blade tip pitch settings within allowable blade stress levels.

The estimated accuracies of the plotted results of the basic quantities measured during the investigation are believed to be within ± 3 percent.

The dynamic twist of the rotor blade was found to be a maximum of about -2.5° at $M_t = 0.75$ (see fig. 3) and was determined by a photographic technique. The accuracy to which the photographed tip angles could be determined was approximately 12 minutes. In order to estimate the dynamic twist distribution, a static moment was applied at the rotor blade tip, and the spanwise blade twist was measured. It was assumed that the dynamic twist would be distributed in a similar manner. For the rotor blade of this investigation, the dynamic twist at the 0.75R station was found to be 42 percent of that at the tip. (See fig. 2.)

Method of Analysis

In rotor research that has been conducted on the Langley helicopter test tower, the principal effect of compressibility and stall has been a rapid increase in profile-drag torque once the critical combination of tip speed and blade angle of attack has been exceeded. A convenient method of determining and evaluating this increase is to take the ratio of the deduced profile-drag torque, from the experimental results, to the calculated profile-drag torque. However, the conventional strip analysis of reference 8 that was found to be successful in predicting the no-stall, hovering performance of uncambered blades at low tip Mach numbers is pessimistic for cambered rotor blades. (See, for instance, ref. 4.) A basic change in the method of analysis is made for this investigation in that the extrapolated $M_t = 0.28$ performance curve of figure 4 is used as the reference for comparison of profile drag.

The calculated rotor performance curve (fig. 4) is based on a linear lift-coefficient slope ($c_l = a\alpha_r$, where $a = 5.73$) and a conventional drag polar ($c_{d,o} = 0.0076 - 0.0216\alpha_r + 0.400\alpha_r^2$). A 3-percent tip-loss factor (outer 3 percent of the blade produces no lift but has profile drag) was used in the calculation.

RESULTS AND DISCUSSION

Results Obtained for Smooth Rotor Blades

The rotor performance and efficiency characteristics for smooth blades are presented in figures 4 to 6. In figure 4 the rotor performance is presented along with a calculated, no-stall curve and a calculated induced-torque-coefficient curve. The extrapolated $M_t = 0.28$ curve is used as the reference curve for determining the profile-drag ratios presented in figures 7 and 8. The low-speed maximum mean lift coefficient of the test rotor is about 1.07 which compares to a value of 1.16 for the rotor having the 15-percent-thick, cambered airfoil of reference 4. This difference can probably be attributed to the smaller leading-edge radius (ref. 9) plus the smaller amount of camber. A more detailed comparison is made in a subsequent section of this paper.

Figure 5 shows the variation of rotor thrust coefficient with blade-section pitch angle for various tip Mach numbers. A calculated curve computed by using a lift-curve slope of 5.73 is plotted along with the actual data for comparison purposes. Generally, the slopes of the curves are similar to those of previous rotor tests; that is, the slope increases above the incompressible slope of 5.73 as the tip Mach number is increased for the range covered.

The effect of tip Mach number on rotor efficiency, expressed as figure of merit, is shown in figure 6. The value of rotor efficiency is above 0.7 for the lift-coefficient and tip speed ranges that utility helicopter designs would be expected to emphasize.

Effects of Tip Mach Number on Profile-Drag Torque Coefficient

The ratios of the deduced profile-drag torque to the reference profile-drag torque are presented as a function of rotor blade tip angle of attack and mean lift coefficient in figures 7 and 8, respectively. The calculations for tip angle of attack are corrected for the measured dynamic twist in the same manner as those previously reported in reference 4. At the lower tip Mach numbers, $M_t = 0.35$ and 0.44, the tip angles for drag divergence (7.7° and 6.2° , respectively) were lower than those of reference 4 (8.6° and 7.5° , respectively). The earlier onset of drag divergence (stall) is attributed to the smaller leading-edge radius and lower camber of the test blades. At the higher tip Mach numbers, however, the tip angles at which drag divergence occurred were higher than those of the thicker rotor blade. This delayed onset shows that the compressibility losses are materially less for this rotor blade, which is the desired result.

The curves of figure 8 indicate that at tip Mach numbers of 0.35 and 0.45 drag divergence occurs at $\bar{c}_l = 0.94$ and 0.83, respectively. For the 15-percent-thick, cambered blade of reference 4, drag divergence occurred at $\bar{c}_l = 0.98$ and 0.90 for $M_t = 0.35$ and 0.43, respectively. The difference in the values of \bar{c}_l for the respective values of M_t substantiates the existence of earlier stall for the airfoil with the thinner leading edge. At the higher Mach numbers ($M_t = 0.65, 0.75$), the rotor reaches a mean lift coefficient of about 0.4 before compressibility losses appear. In the previous test with the 15-percent-thick airfoil, compressibility losses were present at zero mean lift coefficient even at $M_t = 0.65$. Thus, the present airfoil is less susceptible to profile losses at the higher Mach numbers.

Rotor Blade Pitching Moments

The rotor blade pitching-moment coefficients are presented in figure 9 as a function of rotor thrust coefficient. Changes in the blade pitching-moment coefficients as thrust coefficients increase are probably due largely to the chordwise displacement of the blade center of pressure from the blade center of gravity.

The moment data of this figure represent the measured rotor blade moments about the blade pitch axis and include aerodynamic and blade mass forces. Since the actual blade pitching moments were reasonably small (32 to 70 lb-ft), no attempt was made to separate the mass moments from the aerodynamic moments. Abrupt changes in pitching-moment slopes are more significant than the numerical values of the moments. Only at stall, at the lowest tip Mach number, was an abrupt change in pitching moment noted.

Effect of Reduced Thickness and Camber on Figure of Merit

The efficiencies of the rotor of this investigation as a result of reduced thickness and camber are summarized in figure-of-merit form and compared with those of the 15-percent-thick, cambered rotor of reference 4. (See fig. 10.) This figure shows that the rotor of this investigation was about 4 percent less efficient than the rotor of reference 4 for $\bar{c}_l = 0.3$ and values of M_t below 0.52. At the higher tip Mach numbers (0.56 and above), however, the thinner rotor blade achieves better efficiencies than those of the previous investigation. At the higher mean lift coefficients, the efficiencies of the thinner section are slightly less than those of the 15-percent section.

It was noted in reference 10 that a rotor having an NACA 63₂-015 airfoil section averaged hovering efficiencies 2 to 4 percent higher than those of the widely used NACA 0012 airfoil section. The present rotor averages some 6- to 10-percent higher hovering efficiencies than those of the NACA 0012 airfoil. The efficiency decreases quite rapidly in the high-mean-lift-coefficient range as tip Mach number is increased. It does not, however, decrease as rapidly as that of the NACA 0012 airfoil section at the same conditions.

Another rotor, tested on the helicopter tower, having an NACA 0009 tip airfoil section and an NACA 0017 root airfoil section (ref. 5), had an efficiency

in the intermediate mean-lift-coefficient range ($\bar{c}_l = 0.5, 0.7$) that was only 3 to 4 percent less than that of the rotor of this investigation, but exhibited much higher profile-drag power losses at the higher values of \bar{c}_l at Mach numbers often reached by the retreating blade.

Effect of Roughness

Since rotor blades are rarely operated in the smooth condition due to the abrading effects of field operation, three different forms of leading-edge roughness were investigated. First, shellac of rather thick consistency was applied over an area extending along 8 percent of the chord (measured along the surface) back from the leading edge on both the upper and lower surfaces. The resulting spanwise brush marks produced surface waves 0.002 to 0.004 inch in height. Next, the aforementioned condition was replaced with fresh shellac over the same area previously described. The new shellac was sprinkled with 0.005-inch grains of carborundum distributed to cover about 5 percent of the shellaced area. Thirdly, the leading-edge roughness was replaced with a 1/2-inch roughness strip extending from 0.08c rearward on the upper and lower surfaces for the complete span. Measurements of the typical roughness heights showed variations from about 0.006 inch to 0.009 inch. The resulting hovering efficiencies are compared with those for the smooth rotor blade in figure 11. The shellac alone had no distinguishable effect on hovering efficiency, but the standard leading-edge roughness and the further aft 1/2-inch roughness strip caused an approximately 20-percent and 24-percent drop, respectively, in the hovering efficiency for the \bar{c}_l value of 0.3. At a rotor blade mean lift coefficient of 0.9, the standard leading-edge roughness and the 1/2-inch roughness strip caused an approximately 18-percent and 12-percent drop, respectively, in the hovering efficiency.

It should be noted that leading-edge roughness resulted in a greater performance penalty than the rearward roughness strip at the high mean lift coefficient of 0.9, whereas the opposite was found true at the lower mean lift coefficients. This result indicates that, as expected, a smooth leading edge is necessary for best efficiency near stall. The rearward roughness strip, however, does produce a significant performance penalty throughout the mean-lift-coefficient range. A result similar to the effect of rearward roughness can be expected with smooth blades that have a discontinuity between the trailing edge of the leading-edge abrasion strip and the rotor blade.

The efficiency for the rotor investigated with leading-edge roughness was compared with the efficiency of other rotors with roughness added. In this comparison it was found that the present rotor with roughness added, for a \bar{c}_l value of 0.5, was from 2 to 15 percent more efficient than the rotors of references 1, 4, 7, and 11. At a \bar{c}_l value of 0.7 the present rotor was 3 to 18 percent more efficient than the others. As a result of this comparison, together with the previous discussion, it appears that the present rotor would be a desirable choice for a utility type of helicopter.

CONCLUSIONS

The hovering performance characteristics for a full-scale rotor blade having an NACA 63₁A012 airfoil section with an NACA 130 mean line have been determined for the smooth rotor and with leading-edge roughness added. Data for this rotor are compared with data for rotors previously investigated on the Langley helicopter test tower, and in particular with the one having an NACA 63₂A015 airfoil section with an NACA 230 mean line. Examination of the data indicates the following conclusions:

1. The hovering efficiency of a smooth rotor having an NACA 63₁A012 (130 mean line) airfoil section was about 4 percent less than that obtained on the rotor having an NACA 63₂A015 (230 mean line) airfoil section for tip Mach numbers below 0.52 and mean lift coefficients of 0.3. For Mach numbers of 0.56 and up the thinner less cambered rotor realized materially greater efficiency when compared with the thicker more cambered airfoil.

2. The rotor with roughness added was found to be 2 to 15 percent more efficient than other 12- and 15-percent-thick rotors previously investigated with roughness added for a mean lift coefficient of 0.5.

3. The rotor blade pitching moments were relatively small and were nose-up over most of the thrust-coefficient range. The maximum dynamic twist was found to be approximately -2.5° at a tip Mach number of 0.75.

4. It is concluded from the comparisons made that a rotor having an NACA 63₁A012 airfoil section with an NACA 130 mean camber line would give a desirable combination of characteristics for a utility type of helicopter.

Langley Research Center,
National Aeronautics and Space Administration,
Langley Station, Hampton, Va., September 12, 1962.

REFERENCES

1. Shivers, James P., and Carpenter, Paul J.: Experimental Investigation on the Langley Helicopter Test Tower of Compressibility Effects on a Rotor Having NACA 63₂-015 Airfoil Sections. NACA TN 3850, 1956.
2. Loftin, Laurence K., Jr.: Theoretical and Experimental Data for a Number of NACA 6A-Series Airfoil Sections. NACA Rep. 903, 1948. (Supersedes NACA TN 1368.)
3. Lindsey, W. F., and Humphreys, Milton D.: Tests of the NACA 64₁-012 and 64₁A012 Airfoils at High Subsonic Mach Numbers. NACA RM L8D23, 1948.
4. Shivers, James P.: Hovering Characteristics of a Rotor Having an Airfoil Section Designed for Flying-Crane Type of Helicopter. NASA TN D-742, 1961.
5. Powell, Robert D., Jr., and Carpenter, Paul J.: Low Tip Mach Number Stall Characteristics and High Tip Mach Number Compressibility Effects on a Helicopter Rotor Having an NACA 0009 Tip Airfoil Section. NACA TN 4355, 1958.
6. Carpenter, Paul J.: Lift and Profile-Drag Characteristics of an NACA 0012 Airfoil Section as Derived From Measured Helicopter-Rotor Hovering Performance. NACA TN 4357, 1958.
7. Shivers, James P., and Carpenter, Paul J.: Effects of Compressibility on Rotor Hovering Performance and Synthesized Blade-Section Characteristics Derived From Measured Rotor Performance of Blades Having NACA 0015 Airfoil Tip Sections. NACA TN 4356, 1958.
8. Gessow, Alfred, and Myers, Garry C., Jr.: Aerodynamics of the Helicopter. The Macmillan Co., c.1952.
9. Racisz, Stanley F.: Effects of Independent Variations of Mach Number and Reynolds Number on the Maximum Lift Coefficients of Four NACA 6-Series Airfoil Sections. NACA TN 2824, 1952.
10. Dingeldein, Richard C.: Considerations of Methods of Improving Helicopter Efficiency. NASA TN D-734, 1961.
11. Powell, Robert D., Jr.: Compressibility Effects on a Hovering Helicopter Rotor Having an NACA 0018 Root Airfoil Tapering to an NACA 0012 Tip Airfoil. NACA RM L57F26, 1957.

TABLE I.- ORDINATES OF NACA 63₁A012 (130 MEAN LINE) AIRFOIL SECTION

[Stations and ordinates given in percent of airfoil chord]

Upper surface		Lower surface	
Station	Ordinate	Station	Ordinate
0	0	0	0
.361	1.038	.639	-.888
.587	1.272	.913	-1.052
1.053	1.658	1.447	-1.300
2.263	2.397	2.737	-1.731
4.764	3.463	5.236	-2.307
7.312	4.245	7.688	-2.753
9.877	4.843	10.123	-3.141
15.000	5.666	15.000	-3.828
20.058	6.171	19.942	-4.403
25.062	6.492	24.938	-4.836
30.065	6.674	29.935	-5.128
35.066	6.713	34.934	-5.277
40.066	6.620	39.934	-5.294
45.064	6.400	44.936	-5.184
50.061	6.069	49.939	-4.965
55.057	5.646	54.943	-4.650
60.052	5.142	59.948	-4.258
65.046	4.573	64.954	-3.799
70.040	3.952	69.960	-3.290
75.033	3.303	74.967	-2.749
80.027	2.647	79.973	-2.205
85.020	1.992	84.980	-1.660
90.013	1.336	89.987	-1.114
95.007	.680	94.993	-.570
100.000	.025	100.000	-.025

L.E. radius: 1.07
 Slope of radius through L.E.: 0.1527



L-89655

Figure 1.- Typical rotor blade installation on the Langley helicopter test tower.

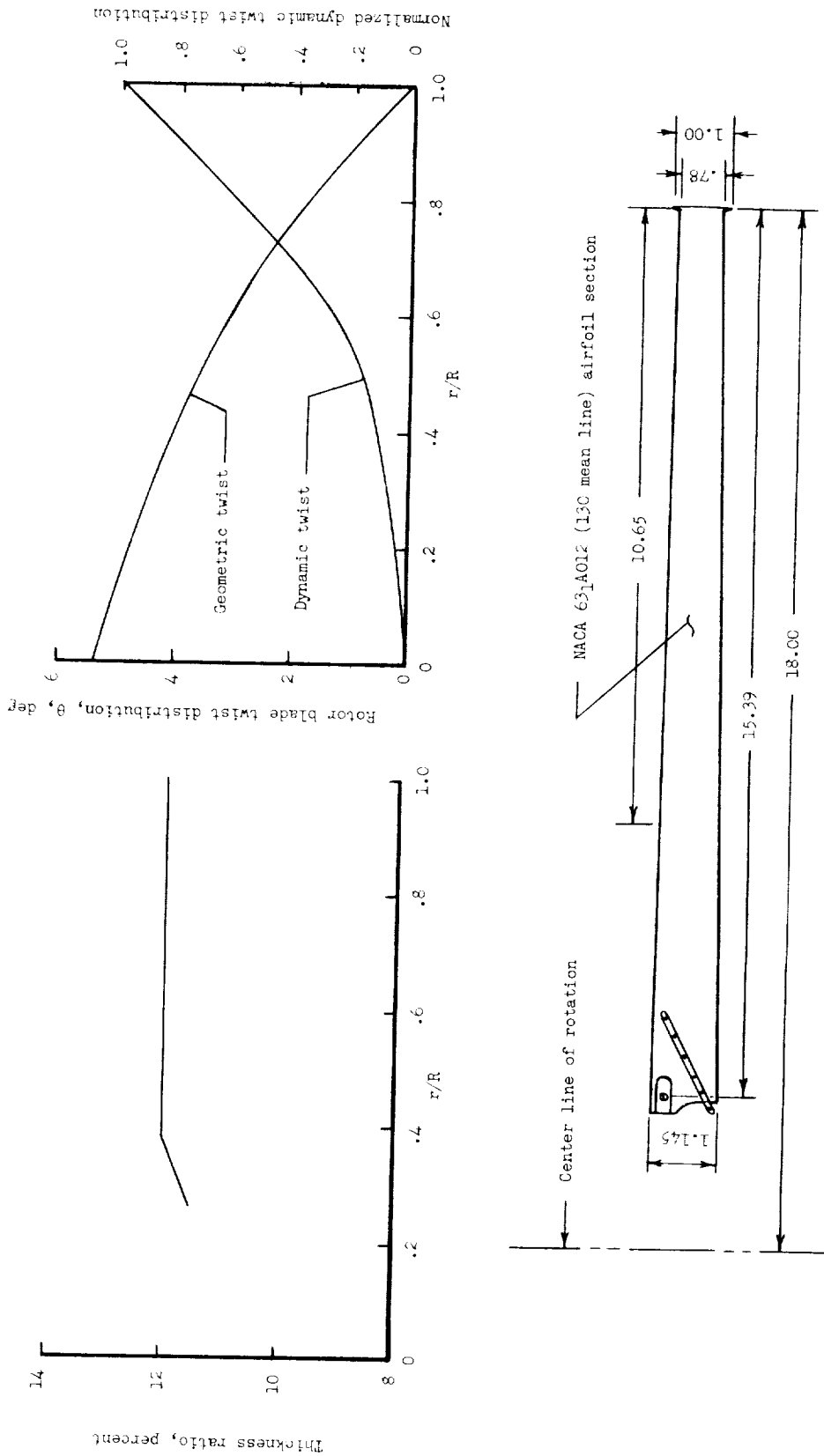


Figure 2.- Sketch of rotor blade having NACA 631A012 airfoil section with a 130 mean line over outer approximate 60 percent of blade radius. Equivalent blade chord = 0.904; $\sigma = 0.032$. All dimensions are in feet.

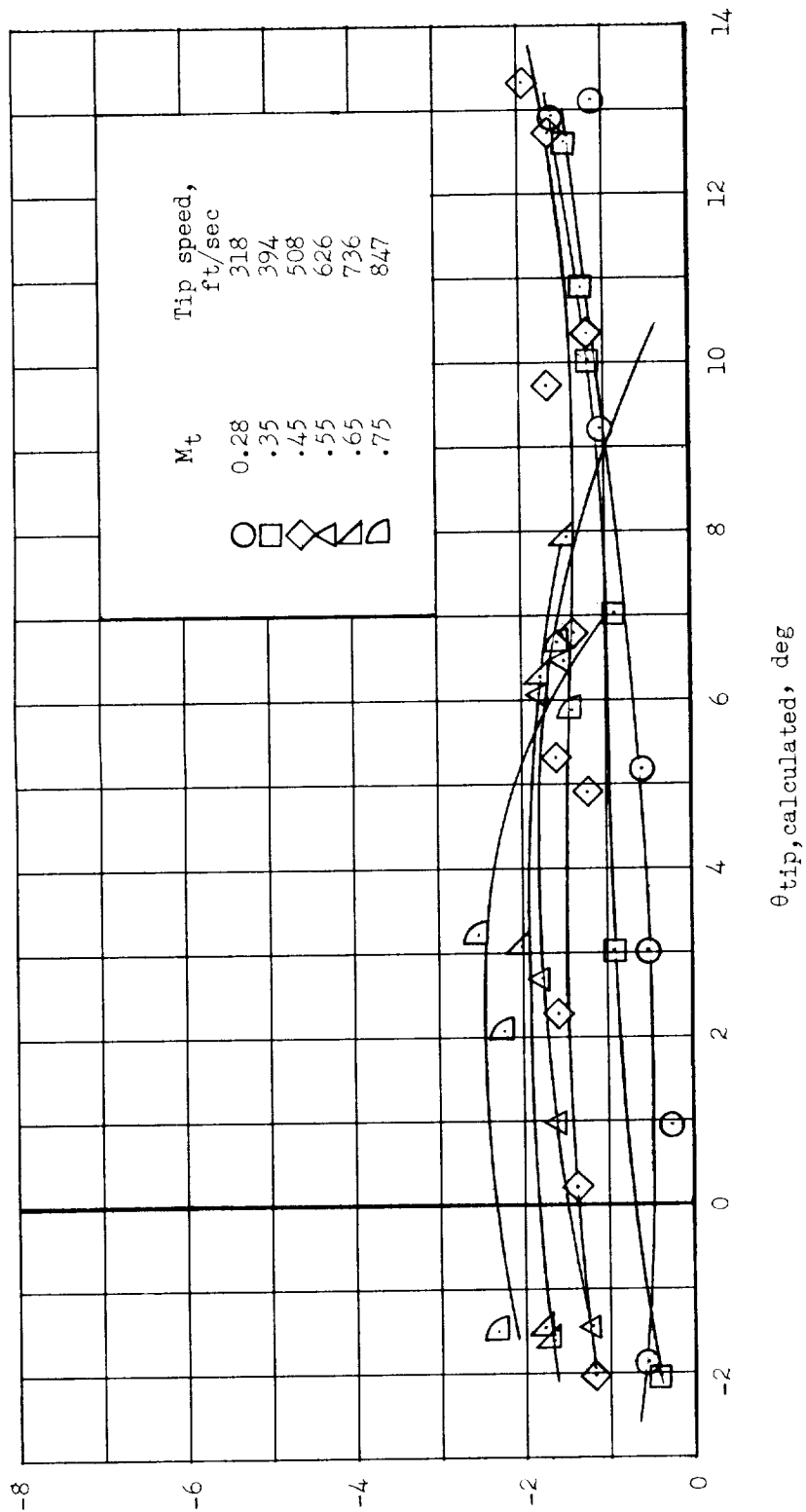


Figure 3.- Effect of tip Mach number on rotor blade dynamic twist.
 $\theta_{tip, calculated} = \theta_{root, measured} + \theta_1$, where θ_1 = geometric twist of rotor blade.

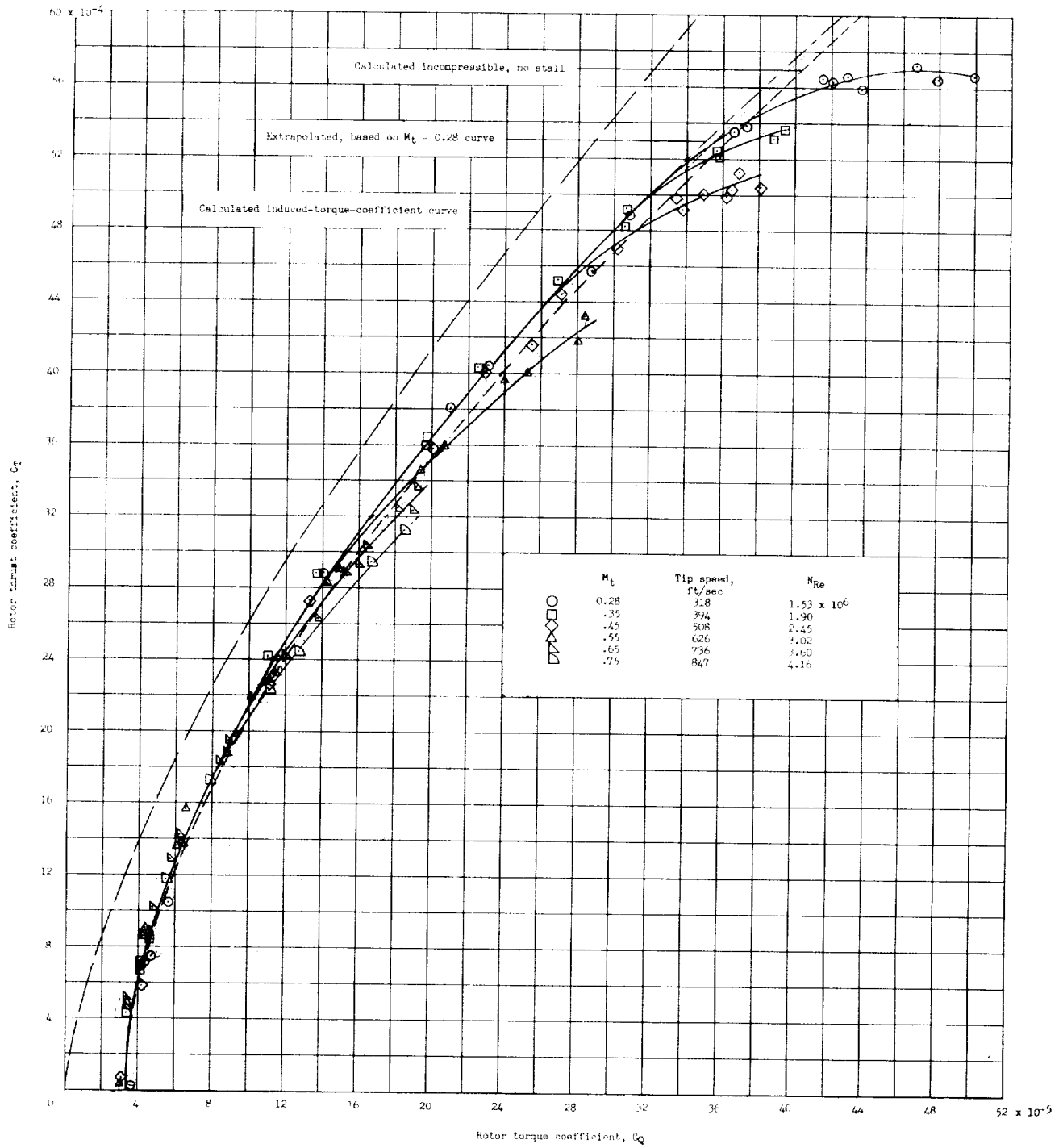
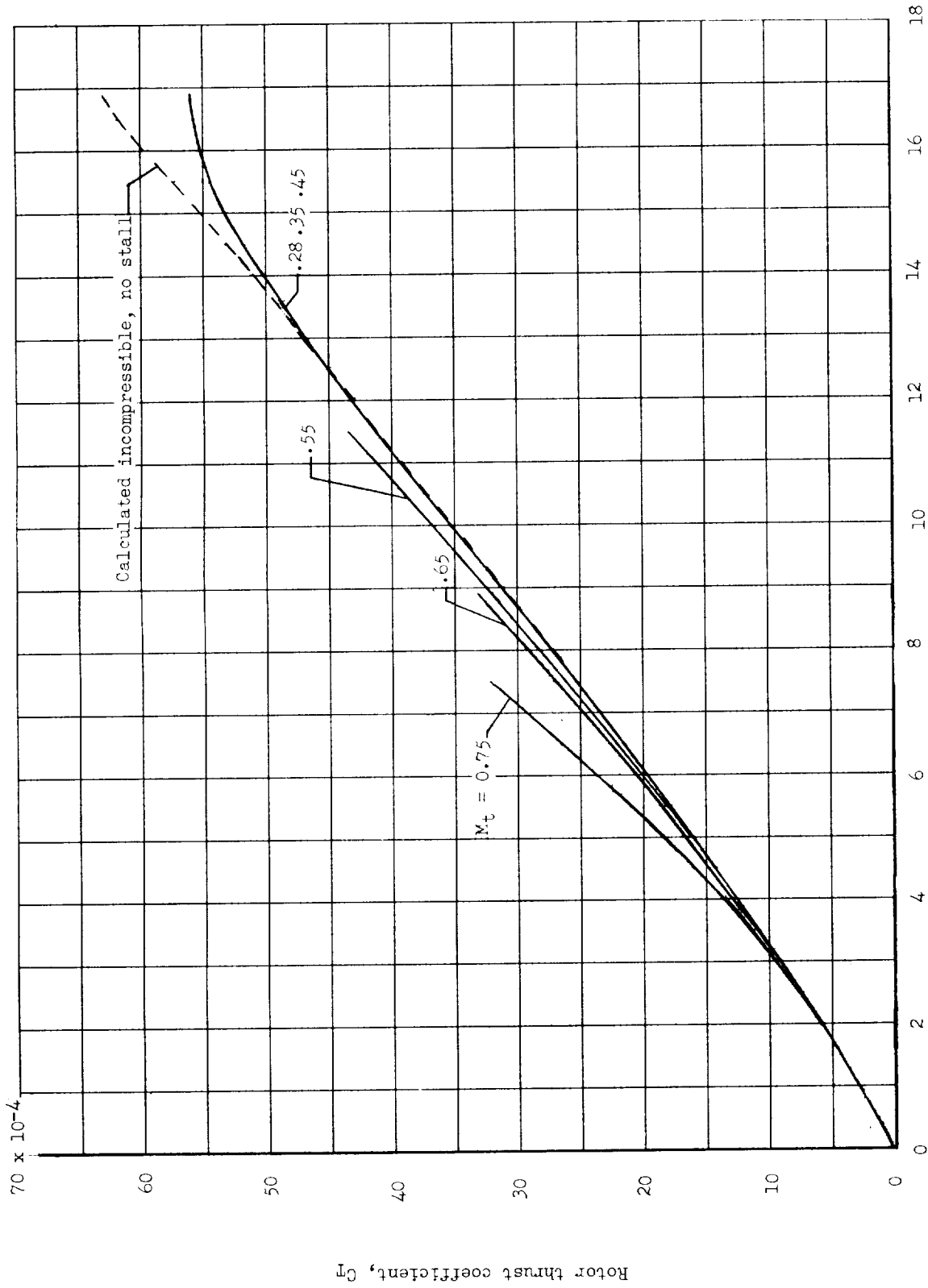


Figure 4.- Hovering performance of rotor blades having NACA 63₁A012 airfoil sections with an NACA 130 mean line. Calculated incompressible curve based on $c_{d,o} = 0.0076 - 0.216\alpha_r + 0.400\alpha_r^2$; $c_l = 5.73\alpha_r$; $\sigma = 0.032$.



Blade section pitch angle measured from zero lift at 0.75R, θ , deg

Figure 5.- Effect of tip Mach number on rotor thrust coefficient.

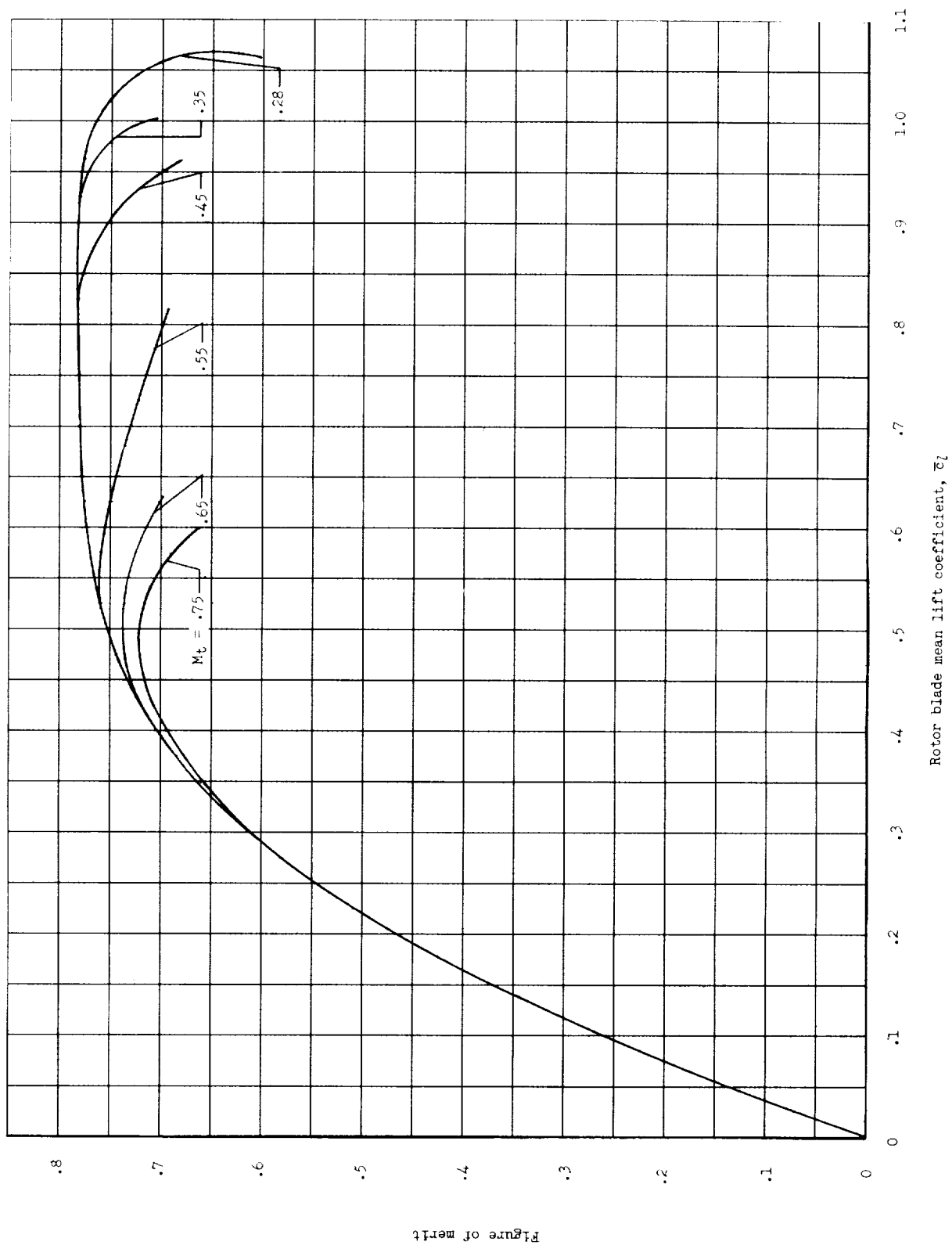


Figure 6.- Effect of tip Mach number on rotor figure of merit.

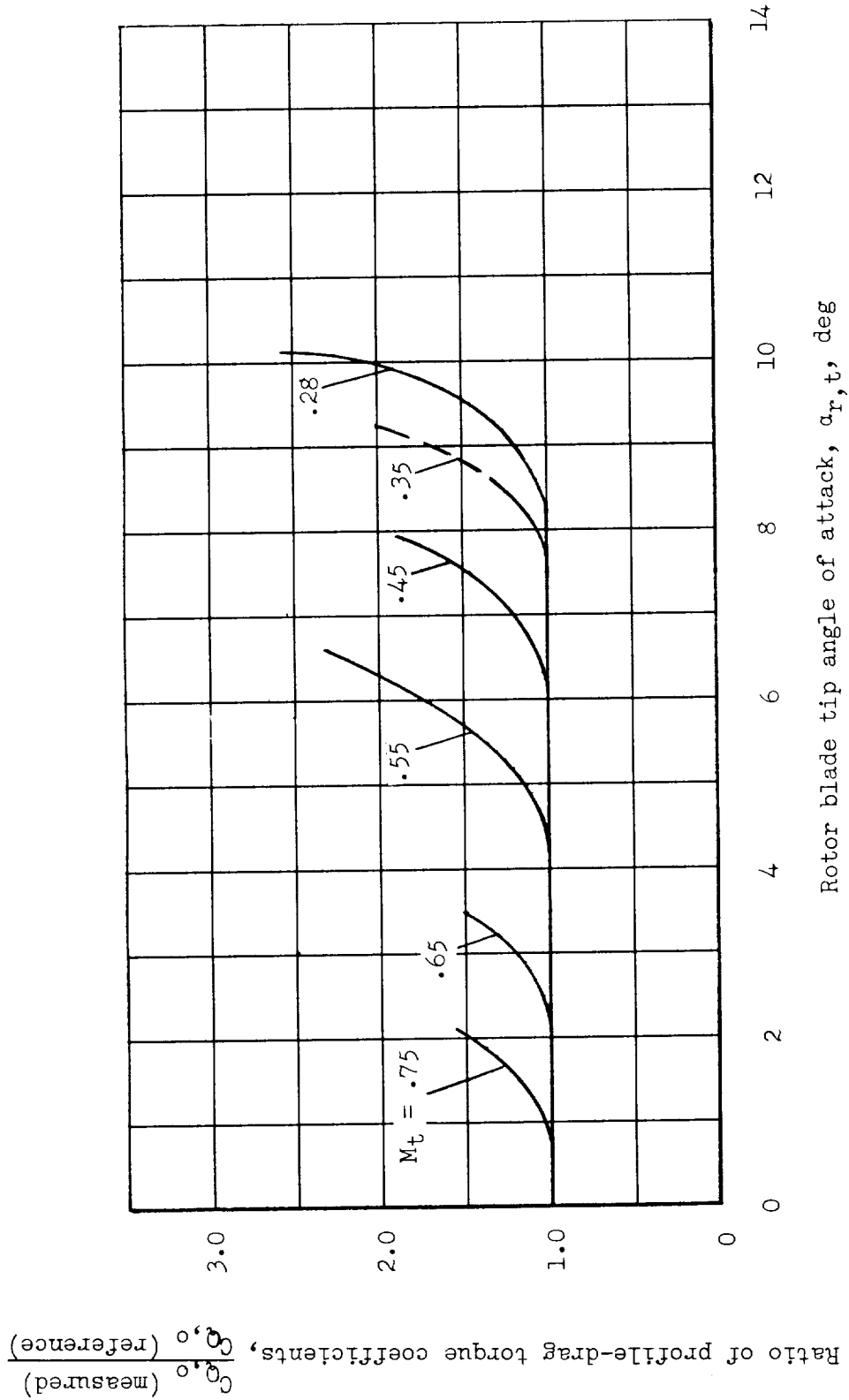


Figure 7.- Effect of tip angle of attack and Mach number on profile-drag torque coefficients. $\alpha_{r,t}$ corrected for dynamic twist. The dashed portion of the curve represents extrapolated data.

Ratio of profile-drag torque coefficients, $\frac{C_{D,0} \text{ (measured)}}{C_{D,0} \text{ (reference)}}$

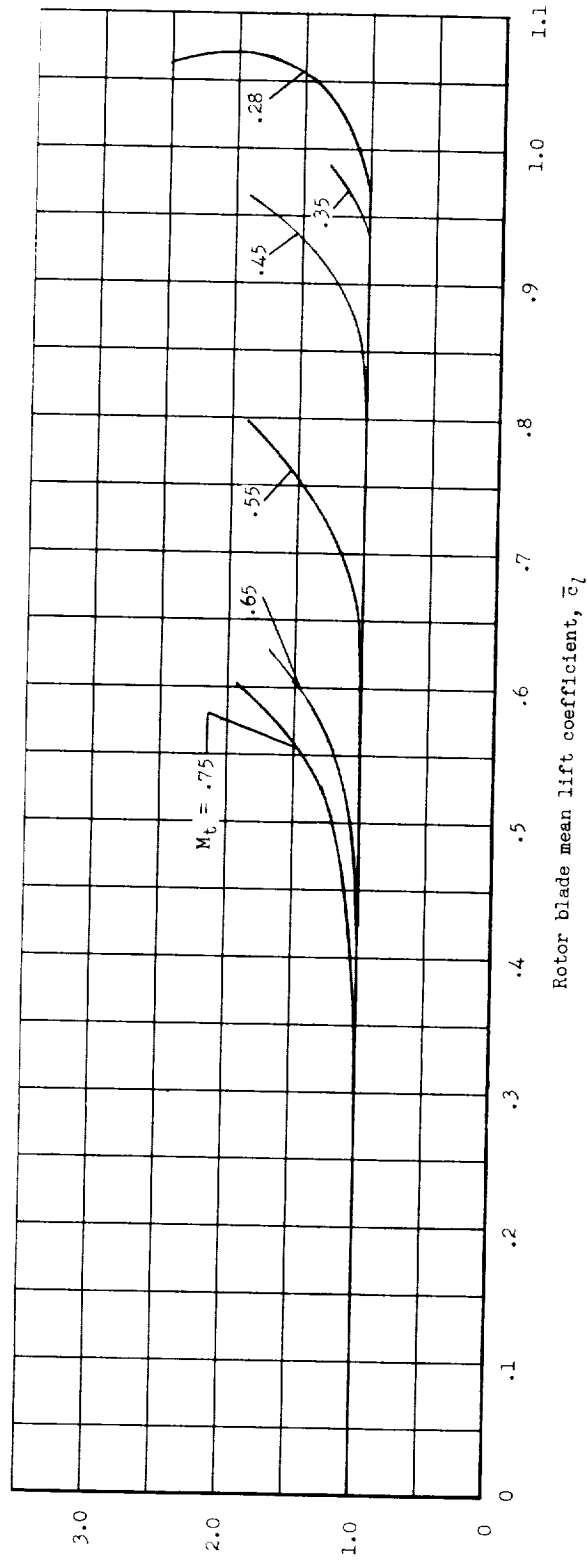


Figure 8.- Effect of rotor blade mean lift coefficient and Mach number on ratio of profile-drag torque coefficients.

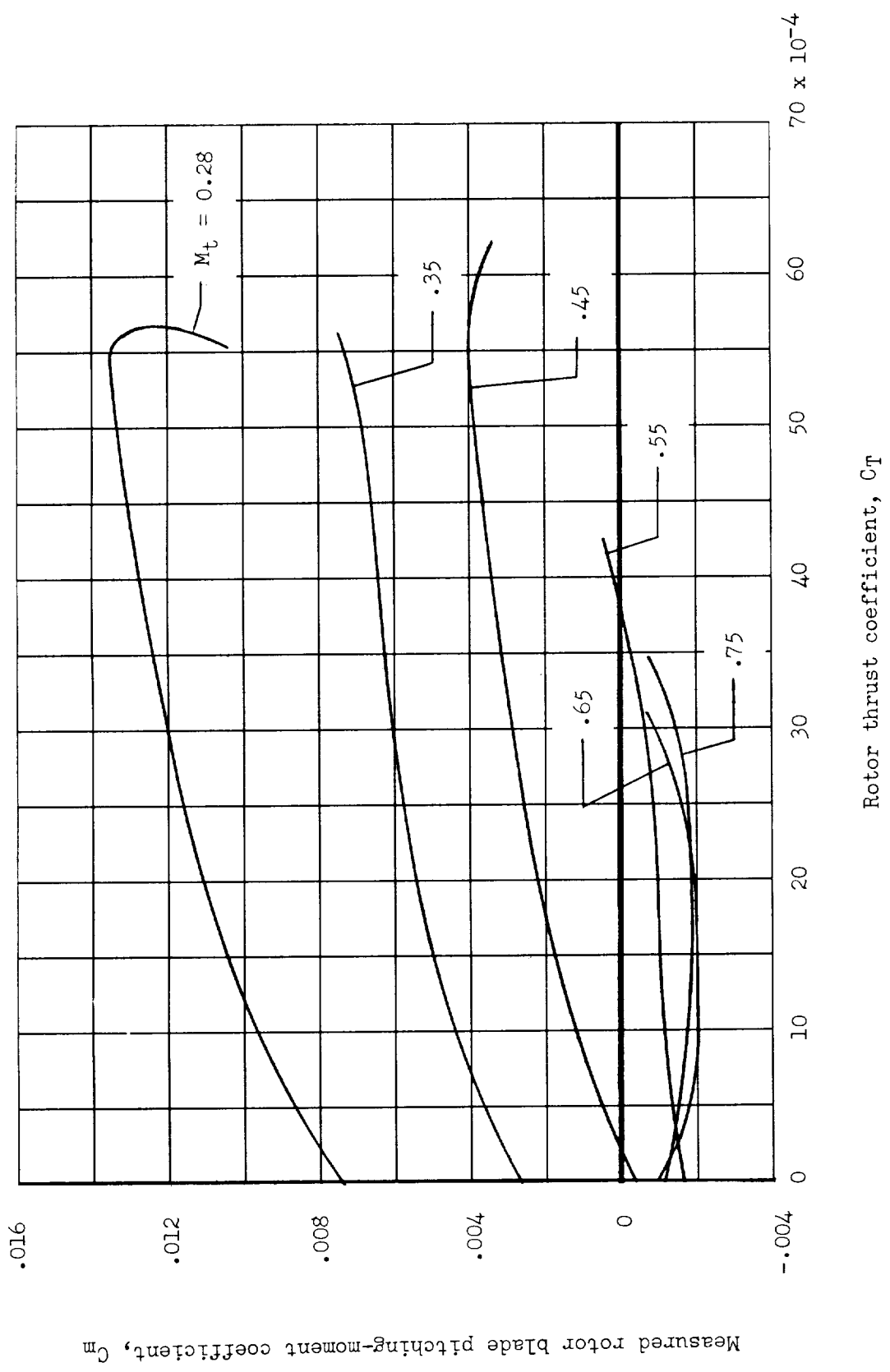


Figure 9.- Effect of tip Mach number on the rotor blade pitching-moment coefficients.

Figure of merit

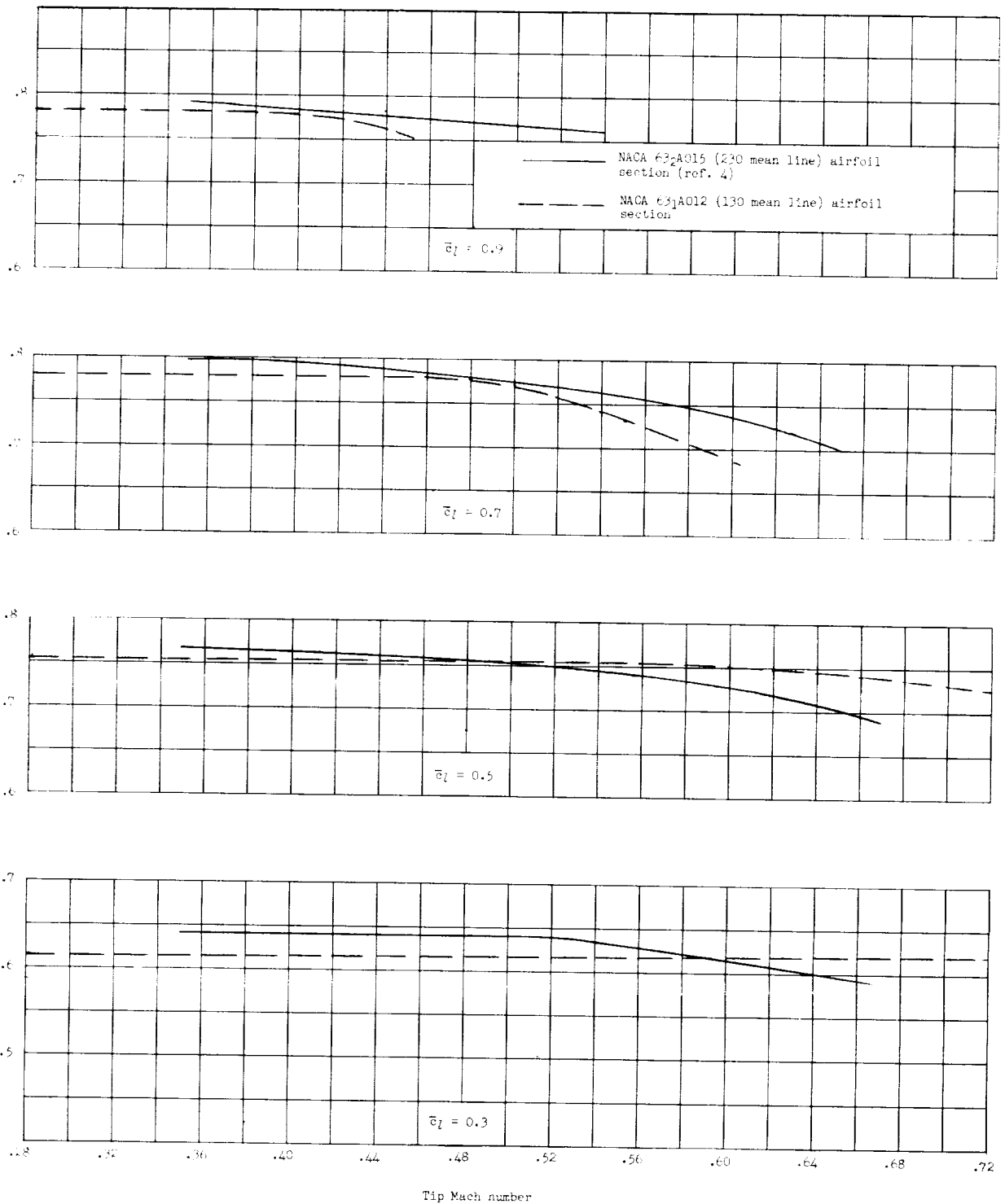


Figure 10.- Comparison of the effects of tip Mach number on rotor efficiency of two NACA airfoils.

Figure of merit

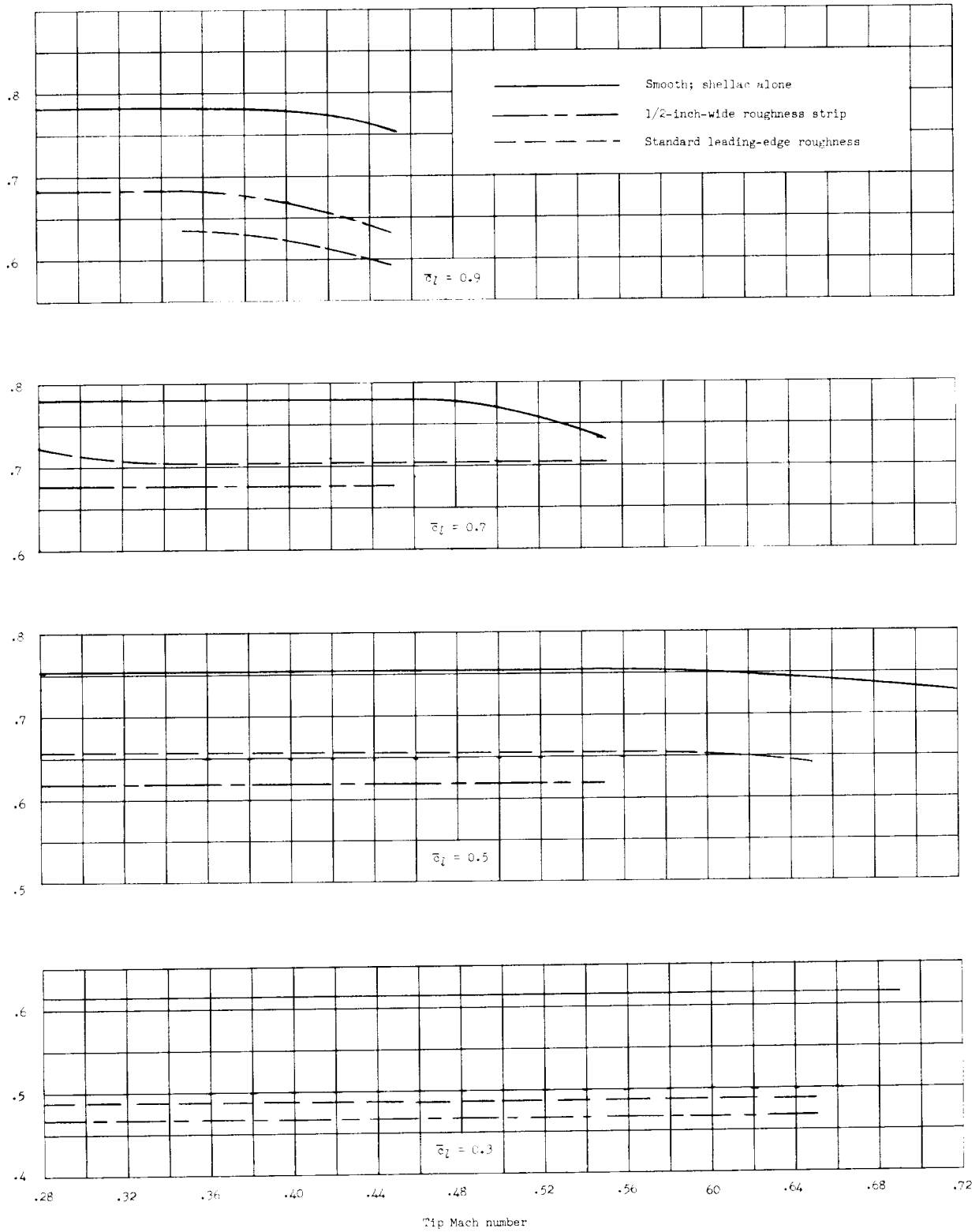


Figure 11.- Effect of leading-edge roughness and tip Mach number on rotor efficiency.